protein–protein interaction. While none of the aromatic protons in g32P shows such a qualitative difference between the two binding modes, the shift of the Tyr^{41} proton in the cooperative g5P complex does show that large upfield shifts in aromatic proton resonances cannot always be associated with ring current shifts induced by the bases of the bound nucleotide. It has also been shown that Leu^{28} of g5P is directly involved in interaction with nucleotide bases (King & Coleman, 1987). Nonaromatic residues of g32P may be candidates for direct interaction with ssDNA, but have not yet been examined.

References

Chase, J. W., & Williams, K. R. (1986) *Annu. Rev. Biochem. 55*, 103.

Coleman, J. E., & Giedroc, D. P. (1989) *Met. Ions Biol. Syst. 25*, 171–234.

Coleman, J. E., Williams, K. R., King, G. C., Prigodich, R. V., Shamoo, Y., & Konigsberg, W. H. (1986) *J. Cell. Biochem. 32*, 305.

Giedroc, D. P., Keating, K. M., Williams, K. R., & Coleman, J. E. (1987) *Biochemistry 26*, 5251.

Giedroc, D. P., Johnson, B. A., Armitage, I. M., & Coleman, J. E. (1989) *Biochemistry 28*, 2410.

Griffith, D. V., Feeney, J., Roberts, G. C. K., & Burgen, A. S. V. (1976) *Biochim. Biophys. Acta 446*, 479.

Keating, K. M., Ghosaini, L. R., Giedroc, D. P., Williams, K. R., Coleman, J. E., & Sturtevant, J. M. (1988) *Biochemistry 27*, 5240.

King, G. C., & Coleman, J. E. (1987) *Biochemistry 26*, 2929.

King, G. C., & Coleman, J. E. (1988) *Biochemistry 27*, 6947.

Korzeniowski, S. H., Blum, L., & Gokel, G. W. (1977) *J. Org. Chem. 42*, 1469.

Kowalczykowski, S. C., Paul, L. S., Lonberg, N. L., Newport, J. W., McSwiggen, J. A., & von Hippel, P. H (1986) *Biochemistry 25*, 1226.

Lonberg, N., Kowalczykowski, S. C., Paul, L. S., & von Hippel, P. H. (1981) *J. Mol. Biol 145*, 123.

Matthews, H. R., Matthews, K. S., & Opella, S. J. (1977) *Biochim. Biophys. Acta 497*, 1.

Ott, D. G. (1981) in *Syntheses with Stable Isotopes of Carbon, Nitrogen, and Oxygen*, p 52, Wiley, New York.

Pan, T., Giedroc, D. P., & Coleman, J. E. (1989) *Biochemistry* (preceding paper in this issue).

Prigodich, R. V., Casas-Finet, J., Williams, K. R., Konigsberg, W., & Coleman, J. E. (1984) Biochemistry *23*, 522.

Prigodich, R. V., Shamoo, Y., Williams, K. R., Chase, J. W., Konigsberg, W. H., & Coleman, J. E. (1986) *Biochemistry 25*, 3666.

Shamoo, Y., Williams, K. R., & Konigsberg, W. H. (1988) *Proteins: Struct., Funct. Genet. 4*, 1.

Shamoo, Y., Ghosani, L. R., Keating, K. M., Williams, K. R., Sturtevant, J. M., & Konigsberg, W. H. (1989) *Biochemistry 28*, 7409.

Spicer, E. K., Williams, K. R., & Konigsberg, W. H. (1979) *J. Biol. Chem. 254*, 6433.

Tuleen, D. L., & Hess, B. A. (1971) *J. Chem. Educ. 48*, 476.

von Hippel, P. H., Kowalczykowski, S. C., Lonberg, N., Newport, J. W., Paul, L. S., Stormo, G. D., & Gold, L. (1982) *J. Mol. Biol. 102*, 795.

A ^{1}H NMR Determination of the Solution Conformation of a Synthetic Peptide Analogue of Calcium-Binding Site III of Rabbit Skeletal Troponin C†

Brian J. Marsden,‡ Robert S. Hodges, and Brian D. Sykes*

Department of Biochemistry and Medical Research Council of Canada Group in Protein Structure and Function, University of Alberta, Edmonton, Alberta, Canada T6G 2H7

Received December 16, 1988; Revised Manuscript Received June 20, 1989

ABSTRACT: NMR techniques have been used to determine the structure in solution of acetyl (Asp 105) skeletal troponin C (103–115) amide, one of a series of synthetic peptide analogues of calcium-binding site III of rabbit skeletal troponin C [Marsden et al. (1988) *Biochemistry 27*, 4198–4206]. The NMR measurements include ^{1}H–^{1}H nuclear Overhauser enhancements and gadolinium-induced ^{1}H relaxation measurements. The former yield short-range internuclear distances (<4 Å); the latter, once properly corrected for chemical exchange, yield longer range metal to proton distances (5–10 Å). These measurements were then used as pseudo potential energy restraints in energy minimization and molecular dynamics calculations to determine the solution structure. Further information was provided by NMR coupling constants, amide proton exchange rates, and the temperature dependences of amide proton chemical shifts. The solution structure of the peptide analogue is very similar to that of the calcium-binding loop in the protein, the root-mean-square deviation between the backbone atoms being ~1.1 Å.

Calcium plays an important role in many biological systems, often acting as a second messenger (Kretsinger, 1980; Seamon & Kretsinger, 1983), where it effects a structural change in regulatory proteins such as troponin C (Ebashi et al., 1968) and calmodulin (Cheung, 1970; Kakiuchi & Yamazaki, 1970). Comparison of the primary sequence of these proteins reveals that the calcium-binding sites consist of highly homologous regions (Barker et al., 1978; Vogt et al., 1979; Reid & Hodges, 1980; Gariépy & Hodges, 1983). Each calcium-binding site exists in a helix–loop–helix arrangement of 31 residues in length; this arrangement has been designated the "EF hand"[1]

† This investigation was supported by a research grant from the Medical Research Council of Canada and an AHFMR fellowship (B.J.M.).

‡ Present address: Division of Biological Sciences, National Research Council Canada, 100 Sussex Drive, Ottawa, Ontario, Canada K1A 0R6.

0006-2960/89/0428-8839$01.50/0

(Kretsinger & Nockolds, 1973). The liganding of the calcium(2+) ion (Ca^{2+}) occurs within the 12-residue loop region. The Ca^{2+} ion is coordinated by the side-chain carboxyl and carbonyl oxygen atoms of Asx and Glu residues at the 1-, 3-, 5-, 9-, and 12-positions as well as the backbone carbonyl of residue 7. These dentates are in an almost octahedral arrangement about the calcium ion, with the residues at positions 1 and 9 occupying the ±X coordinates, 3 and 7 the ±Y coordinates, and 5 and 12 the ±Z coordinates of the cartesian framework (Kretsinger & Nockolds, 1973; Herzberg & James, 1987; Satyshur et al., 1988; Strydnaka & James, 1989).

Since the helix–loop–helix calcium-binding site is derived from as contiguous peptide sequence, the use of synthetic peptide analogues to study this metal binding motif is facilitated. The chemical synthesis of a calcium-binding unit allows specific modifications or substitutions of any residue, and hence the contribution of any residue to the conformation of the site or complexation of the calcium ion to be studied. This approach was first developed by our group using synthetically prepared analogues to study site III of rabbit skeletal troponin C (Reid et al., 1980, 1981; Gariépy et al., 1982) and has since been adopted by other groups to study similar calcium-binding sites (Kanellis et al., 1983; Marchiori et al., 1983; Pavone et al., 1984; Borin et al., 1985; Buchta et al., 1986; Malik et al., 1987). Earlier work by our group has shown that the binding of metal ions to synthetic 13-residue analogues representing just the loop region of a calcium-binding site can be studied by using high-field ^1H nuclear magnetic resonance (NMR) spectroscopy and the combination of NMR and synthesis can be used to probe the events that occur upon binding metal ions in great detail (Gariépy et al., 1983, 1985; Marsden et al., 1987). In particular, we have determined differences in the side chain–cation interaction between Asp and Asn liganding residues by synthesizing analogues that represent all the possible combinations of Asp and Asn at the +X, +Y, and +Z coordinating positions within the loop sequence (Marsden et al., 1988).

The underlying assumption of the synthetic peptide approach is that the peptide–metal complex adopts the same structure as the same sequence has or would have in the protein. In a previous paper, Gariépy et al. (1985) attempted to answer this question for a rabbit skeletal troponin C loop peptide analogue by using ^1H NMR spectroscopy. In that study proton to metal ion distances were determined within the peptide–gadolinium (paramagnetic calcium metal ion analogue) complex from ^1H NMR relaxation time measurements, and the structure was calculated using the distance algorithm developed by Kuntz and co-workers (Crippen, 1981; Havel et al., 1983). The authors were able to demonstrate only that the resulting structure was consistent with the X-ray structure of parvalbumin because of the limited number of distances determined. At that time the X-ray structure of TnC was unknown.

In this paper we present the determination of the structure in solution of the troponin C loop peptide analogue Ac-(Asp105)STnC(103–115) amide complexed to lanthanum (and gadolinium) and compare the structure with that determined by X-ray diffraction methods for turkey and chicken troponin C (Herzberg et al., 1988; Satyshur et al., 1988). Although our approach has been similar in part to that of Gariépy et al. (1985), the improvements over the Gariépy et al. (1985) study are severalfold. With the advent of higher magnetic field strengths for NMR and the further development of two-dimensional NMR methods many more nuclei have been resolved and assigned (Wüthrich, 1986). A particular improvement is that by working in H_2O solutions we have been able to resolve and assign all of the peptide amide NH protons and measure the distance from these nuclei on the peptide backbone to the metal ion. Further, we have used the approach of Lanir and Navon (1972) to separate the contribution of chemical exchange from the measured relaxation times, and also to determine the correlation time for the relaxation, so that the calculated distances are more accurate. Also the 2D NOESY ^1H NMR spectrum, which was used primarily in the assignment of resonances to specific nuclei, also allowed us to determine the nuclear Overhauser enhancements between nuclei and therefore determine a number of internuclear distances, in addition to the metal–nuclei distances determined from NMR relaxation time measurements. The structure in solution has then been calculated by using these distances as pseudo potential energy restraints in energy minimization/molecular dynamics computer algorithms. The resulting structure of the loop peptide in solution is very similar to the X-ray structures of site III of turkey and chicken TnC's in all respects.

Materials and Methods

Materials. Protected amino acid derivatives and other reagents used for the synthesis were described elsewhere (Reid et al., 1981). The lanthanum chloride and gadolinium chloride were obtained from Alfa Inorganics-Ventron (Beverly, MA). Deuterated imidazole was obtained from MSD Isotopes (Montreal, Canada). Deuterium oxide (99.96%) was obtained from Aldrich Chemical Co. (Milwaukee, WI).

Synthesis of Ac(Asp105)STnC(103–115) Amide. The peptide was prepared by solid-phase synthesis on a Beckman 990 peptide synthesizer (Beckman Instruments, Inc., Fullerton, CA) and purified by ion-exchange and reversed-phase HPLC. The synthesis and purification were carried out as described elsewhere (Marsden et al., 1988). The composition and concentration of the pure peptide were determined by amino acid analysis.

Metal Ion Analysis. The solutions of lanthanum and gadolinium were prepared with a solution of 100 mM KCl in 85% H_2O and 15% D_2O and adjusted to pH 5.75 with NaOH or HCl. The metal ion concentrations were determined by EDTA titration using xylenol orange as the end-point indicator (Lee & Sykes, 1980).

Preparation of ^1H NMR Samples. The metal-free spectrum of peptide was recorded with a 18.1 mM sample dissolved in 700 μL of 100 mM KCl in 85% H_2O and 15% D_2O and adjusted to pH 5.75 with NaOH or HCl. The concentration of the peptide was determined by amino acid analysis on three aliquots of 10 μL of the peptide solution removed prior to titration with La^{3+}. The sample was titrated by the addition of small aliquots of a 518 mM $LaCl_3$ solution; the total volume after each addition was 0, 3.3, 5.3, 10.3, 15.3, 20.3, 22.8, 25,3, and 30.3 μL. The ratio of La^{3+}/peptide was 1.2:1 at the end of the titration (an excess of the La^{3+} solution was used to

[1] Abbreviations: Ac(Asp105)STnC(103–115) amide, synthetic N-terminal-acetylated rabbit skeletal troponin C fragment, residues 103–115, with Asp in position 105 and with a C-terminal amide; Boc, *tert*-butyloxycarbonyl; DCC, dicyclohexylcarbodiimide; 2D NMR, two-dimensional nuclear magnetic resonance spectroscopy; DQF COSY, double quantum filtered two-dimensional correlated spectroscopy; EDTA, ethylenediaminetetraacetic acid; "EF hand", Kretsinger's abbreviation of the second calcium-binding domain of carp parvalbumin (this site is thought to represent a typical calcium-binding domain); FID, free induction decay; HOBT, 1-hydroxybenzotriazole; HPLC, high-performance liquid chromatography; NOESY, two-dimensional nuclear Overhauser enhancement spectroscopy; RELAY, two-dimensional related correlation spectroscopy; rms, root mean square; TFA, trifluoroacetic acid; TnC, calcium-binding unit of skeletal muscle troponin; Tos, *p*-toluylsulfonyl.

ensure that the La^{3+}/peptide was 1:1 and that any losses of metal ion due to interaction with the glass matrix would not influence the small concentrations of Gd^{3+} solution to be added later). The Gd^{3+} titration was performed on 20% of the peptide–La^{3+} complex, having a peptide concentration of 3.6 mM and La^{3+} concentration of 4.3 mM, at a temperature of 25 °C. The concentration of the Gd^{3+} solution used was 2.6 mM; eight additions of the solution were made, and the total volume after each addition was 1.0, 2.0, 5.0, 10.0, 15.0, 20.0, 25.0, and 30.3 μL. The composition of the final peptide–metal ion complex was 1:1.2:0.03 peptide/La^{3+}/Gd^{3+}.

Proton NMR Experiments. The ^1H NMR spectra were recorded on a Varian VXR-500 spectrometer. The acquisition parameters used for both the one- and two-dimensional NMR spectra were as follows: sample volume = 700 μL; spectral width = 5800 Hz; 23 360 data points; pulse length = 11.9 μs (≅90°); low-pass filter = ±3000 Hz with quadrature phase detection; number of transients = 128 or 256 for the 1D spectra and 48 or 64 for the 2D spectra; HDO suppression = continuous homonuclear decoupling; internal standard = methyl resonance of 4,4-dimethyl-4-silapentane-1-sulfonate (DSS); resolution enhancement = Lorentzian to Gaussian.

Resonances were assigned to residue type by two-dimensional (2D) relayed coherence transfer (RELAY) spectra (Eich et al., 1982; Bax & Drobny, 1985; Weber et al., 1985) and double quantum filtered coherence (DQF COSY) spectra (Piantini et al., 1982; Rance et al., 1983). Sequential assignments were made by using the 2D nuclear Overhauser enhancement spectroscopy (NOESY) spectra, with mixing periods of 200 and 400 ms. All the 2D experiments were performed at 6 °C to increase the tumbling time of the peptide–La^{3+} complex. The spin–lattice relaxation times (T_1) were determined from standard inversion–recovery experiments. The spin–spin relaxation times (T_2) were determined from the spectra obtained at each titration point by using a line-shape analysis program (CRVFIT, written by Robert Boyko) to determine $\Delta\nu$ and the relationship $\pi(\Delta\nu) = 1/T_2$.

Calculation of Metal–Proton Distances in the Peptide–Metal Ion Complex. When a small fraction (f_M) of the paramagnetic lanthanide Gd^{3+} replaces La^{3+} in the peptide–La^{3+} complex, the increases in the observed relaxation rates of protons of the peptide are made up of contributions from the exchange lifetime of the peptide–Gd^{3+} ion complex, τ_M, and from the paramagnetic contributions to the longitudinal and transverse relaxation times in the complex, T_{1M} and T_{2M}, respectively:

$$\frac{1}{T_{1\,\text{obs-Gd}}} - \frac{1}{T_{1\,\text{obs-La}}} = \frac{f_M}{T_{1P}} = \frac{f_M}{T_{1M} + \tau_M}$$

and similarly for T_{2M}. The equations for T_{1M} and T_{2M} are presented in Gariépy et al., (1985) (eq 3 and 4), along with an expression for the ratio of the relaxation times:

$$\frac{T_{1M}}{T_{2M}} = \frac{7}{6} + \frac{2}{3}\omega_I^2\tau_c^2 = \mathcal{A}$$

Rewriting the right-hand side of $T_{1p} = T_{1M} + \tau_M$, one obtains

$$T_{1p} = \mathcal{A}T_{2p} + \tau_M(1 - \mathcal{A})$$

or

$$T_{2p} = (1/\mathcal{A})T_{1p} + \tau_M(\mathcal{A} - 1)/\mathcal{A}$$

The correlation time of the peptide–metal ion complex, τ_c, and the lifetime of the peptide–metal ion complex, τ_M, are thus determined from the slope and the intercept of the line obtained for a plot of T_{1p} against T_{2p} for the nuclei observed. Once τ_c and τ_M are known, T_{1M} can be obtained from T_{1p} and the metal–nucleus distance r obtained from T_{1M}.

Computer Calculations. All energy minimization and molecular dynamics calculations were made by using the GROMOS Biomolecular Software package provided by Prof. Dr. W. F. van Gunsteren and Prof. Dr. H. J. C. Berendsen of the University of Gröningen in the Netherlands. The pseudo potential energy term used to represent the experimental constraints was of the form

$$k_l(r_l - r)^2 \qquad r < r_l$$

$$k_u(r - r_u)^2 \qquad r > r_u$$

The lower and upper bound distances (r_l and r_u, respectively) and lower and upper bound force constants (k_l and k_u, respectively) used were as follows. (1) For NOE measurements: if $r_{NMR} < 2.5$ Å, then $k_l = 0$ and $r_u = 2.5$ Å; if 2.5 Å $< r_{NMR} < 3.5$ Å then $k_l = k_u$, $r_l = r_{NMR} - 0.5$ Å, and $r_u = r_{NMR} + 0.5$ Å; if $r_{NMR} > 3.5$ Å, then $k_u = 0$ and $r_l = 3.5$ Å. (2) For distances determined from gadolinium relaxation: if $r_{NMR} < 5.0$ Å, then $k_l = 0$ and $r_u = 5.0$ Å; if 5.0 Å $< r_{NMR} < 7.0$ Å, then $k_l = k_u$, $r_l = r_{NMR} - 0.5$ Å, and $r_u = r_{NMR} + 0.5$ Å; if 7.0 Å $< r_{NMR} < 9.0$ Å, then $k_l = k_u$, $r_l = r_{NMR} - 1.0$ Å, and $r_u = r_{NMR} + 1.0$ Å; if $r_{NMR} > 9.0$ Å, then $k_u = 0$ and $r_l = 9.0$ Å.

Molecular mechanics calculations were done for "four picoseconds" at a "temperature" of 300 K.

Results

Assignment of the Resonances. All the experiments used for resonance assignment, including 2D RELAY and NOESY spectra, were performed at a temperature of 6 °C. This temperature was used to increase the rotational correlation time of the peptide–metal complex so that the negative-intensity NOESY cross-peaks were larger, and to ensure that the amide proton resonances were not reduced in intensity due to exchange with the H_2O resonance, which was saturated prior to acquisition of the FID. Partial assignments (excluding the NH protons) have been presented previously (Gariépy et al., 1985; Marsden et al., 1988). The 2D RELAY spectra allowed the resonances of the La^{3+}-bound form of the peptide to be assigned to residue type. The only complete spin systems that were easily identified were those of Gly 108 and the two Ala residues at positions 106 and 112. Integration of the resonances in the region of the spectra that encompasses the amide protons indicated that all 13 of the backbone amides were present at 6 °C, but that overlap of some of the resonances made specific assignments difficult. The NOESY spectra (Figure 1) showed several NH–NH and NH–CH cross-peaks; it was those cross-peaks together with those observed in the RELAY spectra that allowed sequence specific assignments to be made (Wüthrich, 1986). A temperature study of the La^{3+}-bound peptide (Figure 2) showed that most of the overlap was removed at 50 °C, and a 2D RELAY spectra at this temperature removed any ambiguity in assignment of the remaining resonances. The list of assigned resonances is presented in Table I.

Temperature Series. A series of spectra was recorded between the temperatures of 6 and 50 °C to show the effect of temperature on the amide protons of the peptide–La^{3+} complex (Figure 2). At low temperatures all the backbone amide resonances are present as either resolved or overlapping peaks. A number of changes are observed with increasing temperature; these occur in the resolution, chemical shift, and intensity of the amide resonances. In most instances resolution improves, but for those resonances assigned to Ile 110, Glu 113, and Ala 112 both the intensity decreases and the line width

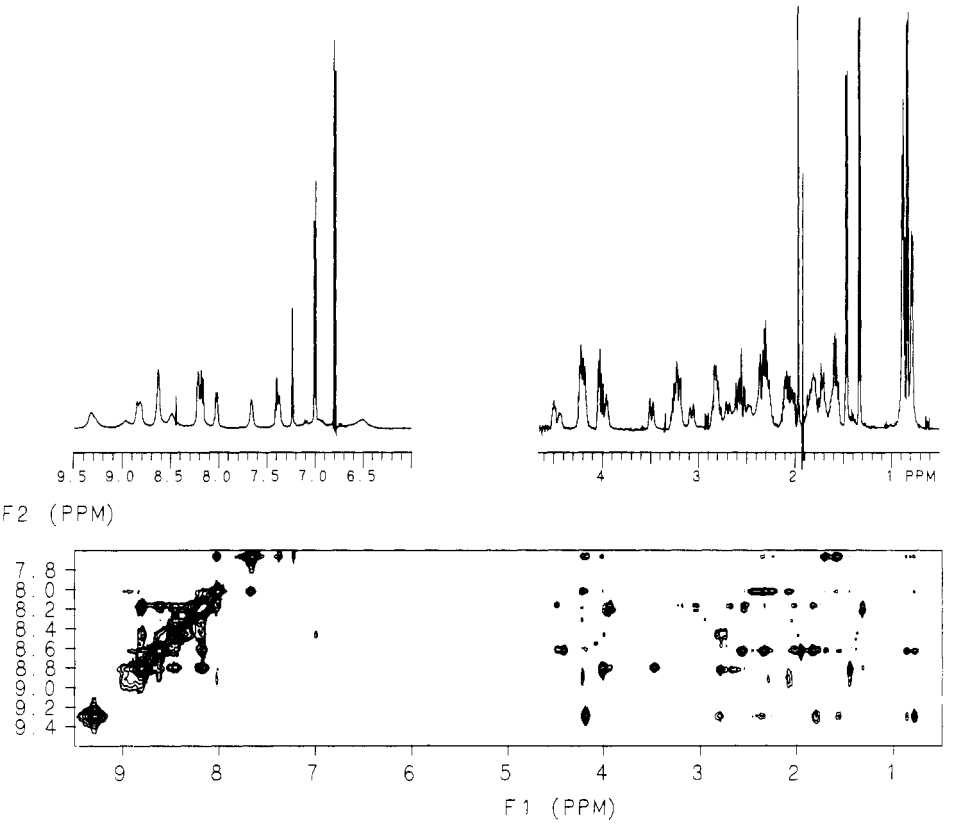

FIGURE 1: Portion of the two-dimensional 500-MHz ^{1}H NMR NOESY spectrum of the Ac(Asp105)STnC(103–115) amide–metal ion complex showing NOE's among the amide NH protons, and between the NH protons and the nonexchangeable CH protons. The peptide concentration was 18.0 mM in 100 mM KCl and 85% H_2O/15% D_2O at 6 °C, pH 5.75. The one-dimensional spectrum is shown above the 2D spectrum for reference.

Table I: Assignment of the ^{1}H NMR Resonances of the La^{3+} Form of Ac(Asp105)STnC(103–115) Amide Analogue at 6 °C[a]

assignment	NH	H^α	H^β	H^γ	H^δ	H^ϵ
Ac		1.97				
Asp 103	8.64	4.43	2.34, 2.58			
Arg 104	8.63	4.49	1.83, 2.03	1.70, 1.80	3.25	7.42
Asp 105	8.17	4.73	2.55, 3.06			
Ala 106	8.23	3.97	1.34			
Asp 107	8.18	4.77	2.70, 3.21			
Gly 108	8.81	3.48, 4.03				
Tyr 109	8.48	4.79	2.78, 2.86	6.80, 6.99		
Ile 110	9.30	4.21	1.81	0.78 (CH_3)	0.87 (CH_3)	
				0.90, 1.41		
Asp 111	9.30		2.66, 2.79			
Ala 112	8.83	4.05	1.47			
Glu 113	8.95	4.23				
Glu 114	8.04	4.25	2.06, 2.30			
Leu 115	7.68	4.19	1.60, 1.72	1.62	0.83 (CH_3)	
					0.87 (CH_3)	

[a] The assignments were made with a combination of RELAY and NOESY spectra recorded in 85% H_2O/15% D_2O. Chemical shifts are given in ppm relative to DSS.

Table II: Fractional Intensities, Temperature Coefficients, and Coupling Constants

amide resonance	fractional intensity at 50 °C[a]	$\Delta\delta/\Delta T$ (ppb/°C[a])	$^3J_{NH-\alpha CH}$ (Hz)[b]	$^3J_{calc}$ (Hz)[c]
Asp 103	0.35	−9.21	5.84	6.1
Arg 104	0.23	−1.92	7.44	4.8
Asp 105	0.31	−1.79	9.39	8.7
Ala 106	0.15	−6.51	5.31	6.9
Asp 107	0.44	−3.94	9.21	7.9
Gly 108	0.28	−1.38		
Tyr 109	0.33	−2.43	9.56	9.6
Ile 110				9.4
Asp 111	0.46	−4.55	8.32	8.3
Ala 112		−8.34		4.2
Glu 113				4.6
Glu 114	0.56	−3.08	8.15	4.9
Leu 115	0.60	−3.08	7.26	

[a] The ratio is equal to twice the area of the NH resonance divided by that of the tyrosine 2,6 protons. [b] The values of $^3J_{calc}$ were determined from the values of the angle ϕ listed for consensus 12-residue loop (Strydnaka & James, 1989), by using the equation $^3J_{NH-\alpha CH} = 6.4\cos^2\theta - 1.4\cos\theta + 1.9$, where $\theta = |\phi - 60°|$, from Pardi et al. (1984). [c] Coupling constants taken from the spectrum at 50 °C.

increases. This may be interpreted as due to increased exchange with solvent.

It is possible to study the exchange properties of the backbone amide protons by measuring the temperature dependency of their relative intensities. This procedure has been used to identify the rapidly exchanging amide protons in peptides of 18 and 19 residues representing the toxic domain of the *Escherichia coli* heat-stable enterotoxin ST 1 (Gariépy et al., 1986). The effect of temperature on intensity and line width is expected to be the same for all protons so any decrease in the relative intensity and broadening of the amide protons with an increase in temperature can be ascribed to exchange with the solvent protons. Gariépy et al. compared intensities of the amide resonances to the nonexchangeable 2,6 ring protons of tyrosine; this approach is only applicable when there are no changes in line width. The spectra in Figure 2 show that there are large changes in line width for many of the amide resonances. This requires that peak integrals and not peak intensities be compared to determine the exchange properties of the amide resonances, but the severe overlap that occurs for many resonances in several of the spectra prevents accurate measurements from being made. The values of peak integrals presented in Table II are the ratios determined at 50 °C where no overlap of resonances occurs.

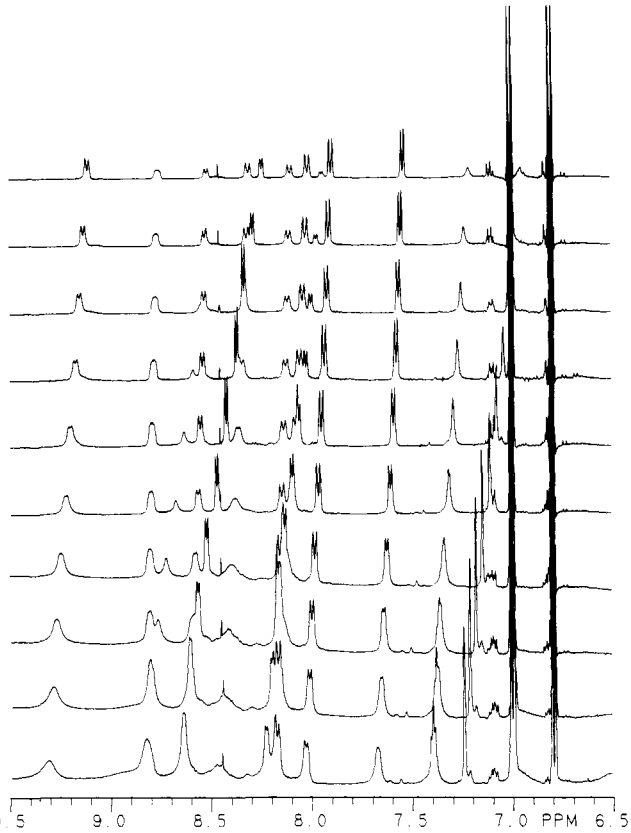

FIGURE 2: Amide NH and aromatic portion of the 500-MHz ^1H NMR spectrum of the Ac(Asp105)STnC(103–115) amide–metal ion complex as a function of temperature (6, 10, 15, 20, 25, 30, 35, 40, 45, and 50 °C, from bottom to top). Peptide concentration was 14.0 mM in 100 mM KCl and 85% H_2O/15% D_2O at 6 °C, pH 5.75. The spectra are scaled to the height of the tyrosine 2.6 proton resonance at 6.99 ppm.

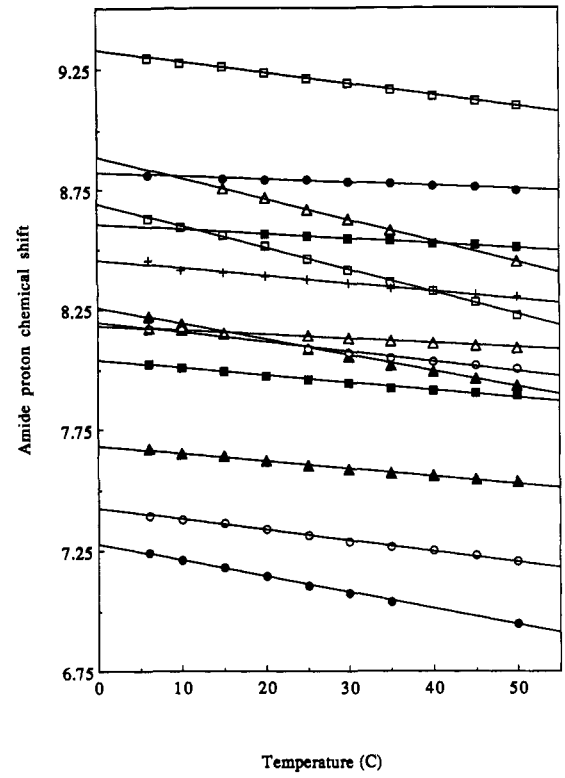

FIGURE 3: Plot of the chemical shifts of the amide NH peptide protons of the Ac(Asp105)STnC(103–115) amide–metal ion complex as a function of temperature. Conditions as in Figure 2. The assignments of the resonances are as follows from low field to high field (i.e. top to bottom) at 50 °C: Asp 111 NH, Gly 108 NH, Arg 104 NH, Ala 112 NH, Tyr 109 NH, Asp 103 NH, Asp 105 NH, Asp 107 NH, Ala 106 NH, Glu 114 NH, Leu 115 NH, Arg 104 ϵNH, and Leu 115 amide NH_2.

The spectra obtained in a temperature study also allow the extent of intramolecular hydrogen bonding to be determined, as the chemical shift of amide protons is temperature dependent. The changes in chemical shift with temperature for the NH resonances are shown in Figure 3, from these plots the temperature coefficients $\Delta\delta/\Delta T$ of the amide protons of the peptide–lanthanum complex were calculated and are listed in Table II.

At the higher temperatures where the amide resonances are generally more well resolved, the NH–αCH coupling constants can be measured. These reflect the values of the dihedral angle ϕ and are also listed in Table II.

Calculation of Internuclear Distances. The volume integrals of the assigned NOE cross-peaks shown in Figure 1 are presented in Table III. These were converted to internuclear distances (r_{ij}) between nuclei i and j after normalizing for the number of protons i and j involved (n_i and n_j) by dividing by the factor $(n_i n_j)/(n_i + n_j)$ (Williamson & Neuhaus, 1987). The distances were obtained by using the two-spin approximation

$$r_{ij} = (\mathrm{NOE}_{\mathrm{REF}}/\mathrm{NOE}_{ij})^{1/6} r_{\mathrm{REF}}$$

with the Tyr 109 ring protons (2 ↔ 3 and 5 ↔ 6) used as the reference distance (see Table III). The two-spin approximation was considered valid in this case even with the long mixing times used since cross relaxation is relatively ineffective near $\omega_1\tau_c = 1$ (Sykes et al., 1978).

Gadolinium Titration. The spectra obtained during the titration of the La^{3+}-bound form of the peptide with Gd^{3+} are shown in Figure 4. The effect of the Gd^{3+} ion on the proton resonances is seen clearly. The changes in resonance line width due to the presence of the paramagnetic ion can be related to the metal ion–proton distance. The βCH_2 protons of Asp 103, 105, 107, and 111, the γCH_2 protons of the Glu 113 and 114, and the αCH proton of Tyr 109 can be seen to broaden at a greater rate than any other protons, as would be expected for protons that are closest to metal coordinating centers. Spin–lattice relaxation times (T_1) and spin–spin relaxation times (T_2) were determined for all the resonances that did not suffer any overlap, and they display similar trends. The values of $1/T_{1p}$ and $1/T_{2p}$ determined for individual resolved and assigned resonances are shown in Table IV.

Discussion

In this study we present the determination of the structure in solution of the troponin C loop peptide analogue Ac-(Asp105)STnC(103–115) amide, representing site III of rabbit skeletal troponin C, complexed to lanthanum (and gadolinium). The approach we have used in similar in part to that of Gariépy et al. (1985), but by performing the experiments in H_2O solutions we have been able to resolve and assign all of the peptide amide NH protons and most of the side-chain protons. It is apparent in Figure 4 that differential broadening of the resonances occurs during the titration with Gd^{3+} and that the resonances of Asp residues 103, 105, 107, and 111 which are associated with coordination to the metal ion broaden faster than most of those protons that are not associated with coordination of the metal ion, such as the methyl resonances of the *N*-acetyl, Ala 106 and 112, Ile 110, and Leu 115 residues.

To determine the metal–nuclei distances, r, from these relaxation measurements, T_{1p} and T_{2p}, it is necessary to known the correlation time for the interaction of the peptide and metal

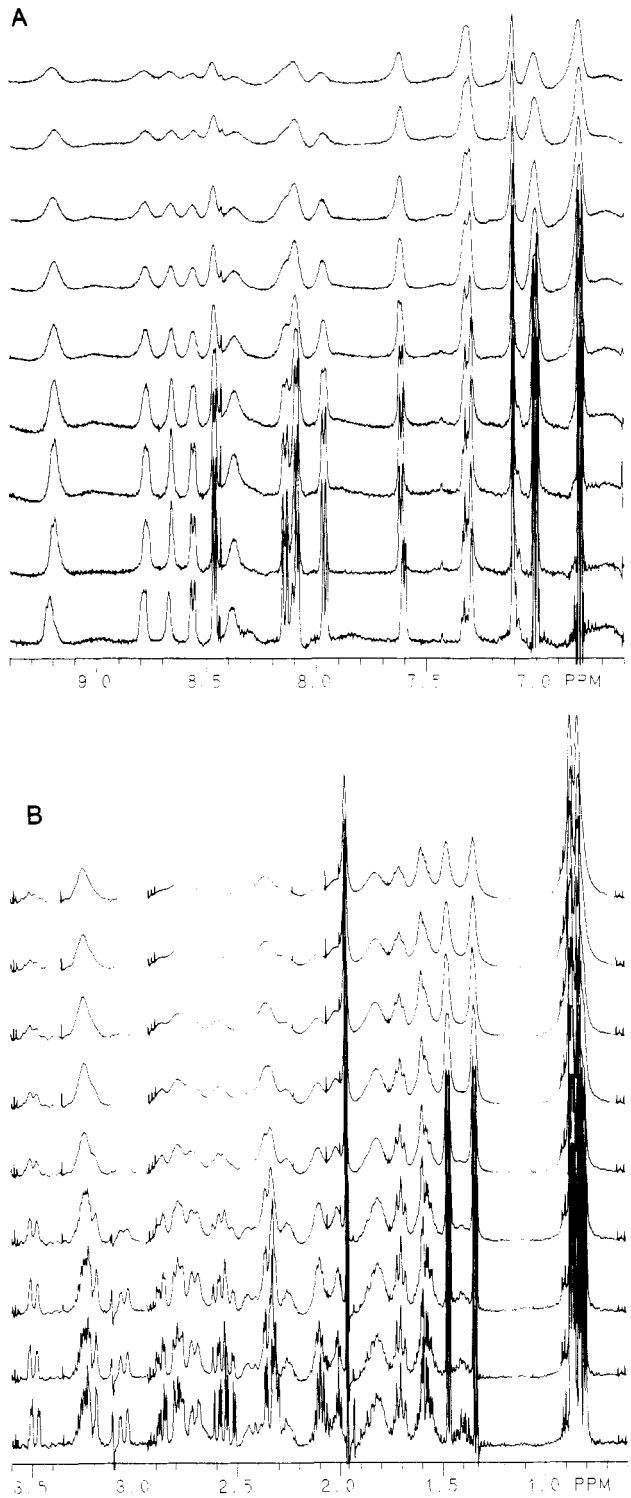

FIGURE 4: Amide and aromatic portion (A) and aliphatic portion (B) of 500-MHz ^{1}H NMR spectrum of the Ac(Asp105)STnC(103–115) amide–lanthanum ion complex as a function of added gadolinium ion. Peptide concentration was 3.6 mM in 100 mM KCl in 85% H_2O/15% D_2O at 25 °C, pH 5.75. The concentration of gadolinium in percent of total peptide–lanthanum complex is (from bottom to top) 0, 0.1, 0.2, 0.5, 1.0, 1.5, 2.0, 2.5, and 3.0. Spectra were scaled to the height of methyl resonances of DSS. The vertical scale of spectra A is 2.5 times that of spectra B.

ions and to separate the contribution of chemical exchange (τ_M) from that of T_{1m} and T_{2m}, respectively. This is accomplished by plotting the measured values of T_{2p} versus T_{1p} (see Figure 5) for all resolved and assigned resonances (Lanir & Navon, 1972). The slope of this plot (defined as $1/\mathcal{A}$) is 0.23, which yields a value for τ_c of 0.70×10^{-9} s (see Materials and

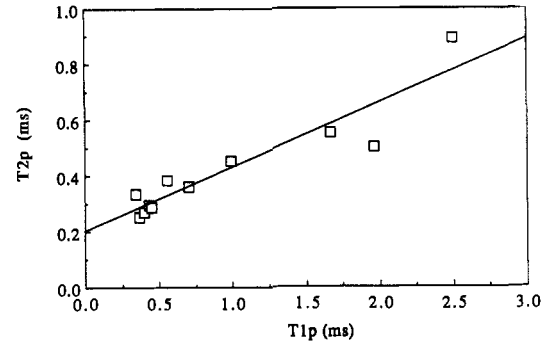

FIGURE 5: Plot of T_{2p} versus T_{1p} for assigned resonances (see Table IV) of the Ac(Asp105)STnC(103–115) amide–gadolinium complex at pH 5.75, 25 °C, in 100 mM KCl and 85% H_2O/15% D_2O.

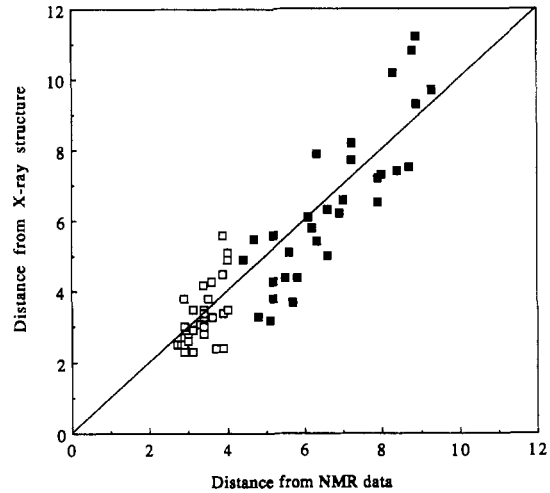

FIGURE 6: Plot of distances calculated from NMR data versus equivalent distances deduced from X-ray structure of Herzberg and James (1987). Proton–proton distances determined from NOE's are indicated by □; proton–metal distances determined from relaxation measurements are indicated by ■.

Methods). This value is close to that expected for the rotational correlation time of this complex and yields a value of $\omega_I\tau_c = 2.2$. This is just slightly larger than 1, as expected for the fact that no NOE's are observed at 25 °C, and small negative NOE's are observed at 6 °C. The intercept in Figure 5 [defined as $\tau_M(\mathcal{A} - 1)/\mathcal{A}$; see Materials and Methods] is 2.0×10^{-4}. By use of the value of $\mathcal{A} = 4.4$ from above, a value of $\tau_M = 2.6 \times 10^{-4}$ s was determined. With this value for τ_M it was possible to separate all of the T_{1p} measurements into τ_M and T_{1m}; the values of T_{1m} and that of τ_c were then used to calculate the distances r, which are listed in Table 4.

The metal to nuclei distances determined from the relaxation measurements in the presence of Gd^{3+} (Table IV), and the internuclear distances determined from the NOE measurements (Table III), can be compared to the distances implied from the X-ray structure. To make the comparison, the X-ray structure of turkey TnC was modified to include protons, the positions of which were calculated from standard bond lengths and bond angles. The "X-ray" distances were then determined from as closely equivalent protons as possible, since the sequences are not identical, and these are listed in Tables III and IV. The distances determined from NMR in solution are compared to the closest equivalent protons calculated from the X-ray structure in Figure 6. The rms deviation between the two data sets is 1.1 Å. This is considered quite good since there is no reason that all protons will be in the same conformation in the peptide and in the protein. Consider, for example, the Ile side chain, which is exposed to solution in the peptide but buried in the core of the protein. These data are thus con-

Table III: Volume Integrals of Assigned Cross-Peaks in NOESY Spectrum, Calculated ^1H–^1H Distances in the Peptide, and Equivalent Distances in the X-ray Structure

nucleus *i*		nucleus *j*	vol NOE	*r* (NMR) (Å)	*r* (X-ray) (Å)	eqiuv *i*		equiv *j*
103 Asp NH	↔	102 NAc CH_3	33.3	2.8	2.5	106 Asp NH	↔	105 Phe αCH
104 Arg NH	↔	104 Arg βCH	16.5	2.9	2.7	107 Lys NH	↔	107 Lys βCH
104 Arg NH	↔	104 Arg βCH′	18.1	2.9	3.8	107 Lys NH	↔	107 Lys βCH′
104 Arg NH	↔	104 γCH	6.7	3.4	3.8/2.2	107 Lys NH	↔	107 Lys γCH
105 Asp NH	↔	104 Arg αCH	6.9	3.4	3.5	108 Asp NH	↔	108 Lys αCH
105 Asp NH	↔	104 Arg βCH	6.7	3.4	3.3	108 Asp NH	↔	108 Lys βCH
105 Asp NH	↔	104 Arg βCH′	6.5	3.4	4.2	108 Asp NH	↔	108 Lys βCH′
105 Asp NH	↔	104 Arg γCH	2.3	4.0	5.5/4.6	108 Asp NH	↔	108 Lys γCH
106 Ala NH	↔	106 Ala CH_3	16.1	3.1	3.5	109 Ala NH	↔	109 Ala CH_3
107 Asp NH	↔	106 Ala CH_3	4.5	3.9	4.5	110 Asp NH	↔	109 Ala CH_3
107 Asp NH	↔	107 Asp βCH	7.5	3.3	3.1	110 Asp NH	↔	110 Asp βCH
107 Asp NH	↔	107 Asp βCH′	5.0	3.5	3.8	110 Asp NH	↔	110 Asp βCH′
108 Gly NH	↔	106 Ala αCH	4.9	3.6	4.3	111 Gly NH	↔	109 Ala αCH
108 Gly NH	↔	106 Ala CH_3	3.8	4.0	4.9	111 Gly NH	↔	109 Ala CH_3
108 Gly NH	↔	108 Gly αCH	17.1	2.9	3.0	111 Gly NH	↔	111 Gly αCH
108 Gly NH	↔	108 Gly αCH′	25.1	2.7	2.5	111 Gly NH	↔	111 Gly αCH′
108 Gly NH	↔	109 Tyr NH	9.3	3.2	2.4	112 Gly NH	↔	112 Phe NH
109 Tyr NH	↔	108 Gly αCH	4.7	3.6	3.3	112 Phe NH	↔	111 Gly αCH
109 Tyr NH	↔	108 Gly αCH′	2.8	3.9	3.4	112 Phe NH	↔	111 Gly αCH′
109 Tyr 2,6	↔	109 Tyr 3,5	90.0[a]	[2.46]	2.46	112 Phe 2,6	↔	112 Phe 3,5
109 Tyr NH	↔	110 Ile γCH	4.1	3.9	5.2/5.9	112 Phe NH	↔	113 Ile γCH
112 Ala NH	↔	111 Asp βCH	15.3	2.9	2.3	115 Ile NH	↔	114 Asp βCH
112 Ala NH	↔	111 Asp βCH′	15.3	2.9	3.8	115 Ile NH	↔	114 Asp βCH′
112 Ala NH	↔	112 Ala CH_3	15.7	3.1	2.3	115 Ile NH	↔	115 Ile βCH
113 Glu NH	↔	112 Ala CH_3	9.5	3.4	3.4	116 Glu NH	↔	115 Ile βCH
113 Glu NH	↔	114 Glu NH	6.9	3.4	2.8	116 Glu NH	↔	117 Glu NH
114 Glu NH	↔	114 Glu αCH	11.7	3.1	2.9	117 Glu NH	↔	117 Glu αH
114 Glu NH	↔	115 Leu NH	13.0	3.0	2.7	117 Glu NH	↔	117 Leu NH
115 Leu NH	↔	114 Glu βCH′	2.4	4.0	3.5	118 Leu NH	↔	117 Glu βCH
115 Leu NH	↔	114 Glu βCH′	2.8	3.9	2.4	118 Leu NH	↔	117 Glu βCH′
115 Leu NH	↔	115 Leu αCH	11.0	3.1	2.9	118 Leu NH	↔	118 Leu αCH
115 Leu NH	↔	115 Leu βCH	12.8	3.0	2.6	118 Leu NH	↔	118 Leu βCH
115 Leu NH	↔	115 Leu βCH′	16.3	2.9	2.5	118 Leu NH	↔	118 Leu βCH′

[a] To obtain distances, all volume integrals were normalized by the factor $n_i n_j/(n_j + n_j)$ (see text). For Tyr 2,6 ↔ 3,5 NOE, $n_i = n_j = 2$.

sidered as a strong indication that the structure of the peptide in solution is very similar to that in the protein.

To determine the structure in solution, the distances determined by NMR were used as pseudo potential energy restraints in energy minimization and molecular dynamics computer calculations (see Materials and Methods). On the basis of Figure 6, the X-ray structure was chosen as the starting structure for these calculations after it was modified to the proper amino acid sequence by using the program MUTATE, written by Dr. Randy Reid, and the N-terminal acetyl group and the C-terminal amide group were added. This structure was then subjected to energy minimization with the distance restraints included, followed by molecular dynamics also in the presence of the distance restraints. These calculations were performed with the in vacuo force field included in the GROMOS software package since no solvent molecules were included in the calculation. The rms residual distance violations of the average of three molecular mechanics structures relative to the experimental restraints were ± 0.2 Å.

Presented in Figure 7A is a superposition of the peptide backbone of the X-ray structure and that of three molecular dynamics structures which have been translated to superimpose the calcium ions. One can see in this figure that these structures are very similar; see, as an example, the magnitude of the variation in position of the liganding carbonyl oxygen at the −Y position of the calcium coordination sphere. A comparison of the X-ray structure and the average of the molecular dynamics structures is shown in Figure 7B, with the side chains of the liganding residues included. The rms difference between the two structures in Figure 7B is 1.8 Å when all of the atoms are included and 1.1 Å when only the backbone is included. This is due, in part, to the fact that some of the side chains are on the outside of the peptide but would be on the inside of the protein.

Some further comparison of the solution structure of the peptide–metal complex with the structure of the loop in the protein can be made on the basis of the coupling constants presented in Table II. These reflect the dihedral angle θ, which is in turn related to the angle ϕ ($\theta = |\phi - 60°|$). Since the coupling constant does not uniquely define a single angle ϕ, but the reverse equation is single valued, we have compared the observed coupling constants with those calculated from the ϕ angles of a consensus calcium-binding site (Strydnaka & James, 1989). Taking into account experimental errors in the measurements and the equation relating angle to coupling constant, the comparison with a consensus loop, and the additional fact that the coupling constants were measured at 50 °C, the correspondence is quite good especially for residues in the middle of the loop such as Tyr 109 and Asp 111. To give an idea of the change in angles involved, for Asp 107 the consensus $\phi = -90°$ corresponds to $^3J = 7.9$ Hz. A change in ϕ to $-105°$ produces the value of 9.2 Hz for ^3J, which is that observed. Similarly, for Arg 104 a change in ϕ of 20° will bring the calculated and observed coupling constants into agreement.

Further information about the solution structure can be obtained from the temperature coefficients of the NH resonances. Only the NH resonances of Asp 103, Ala 106, and Ala 112 show the characteristic temperature dependence expected for completely exposed amide protons as found in a random coil. The temperature coefficients of random coil amide protons in H_2O are expected to range from -6×10^{-3} to -1×10^{-2} ppm/°C (Deslauriers & Smith, 1980). The reduced temperature coefficients of the NH resonances of Arg 104, Asp 105, Asp 107, Gly 108, Tyr 109, Asp 111, Glu 114,

Table IV: Values of Slopes Determined from Gadolinium-Induced Relaxation Plots, Calculated Metal-^{1}H Distances, and Equivalent Distances in the X-ray Structure

nucleus of (Asp105)-STnC(103-115) amide	$1/T_{1p}$	$1/T_{2p}$	r (NMR) (Å)	r (X-ray) (Å)	equiv nucleus of turkey TnC
102 NAc CH_3	400	1120	8.7	7.5	105 Phe αCH
103 Asp NH	1430	2780	6.6	6.3	106 Asp NH
103 Asp βCH	1390		6.6	5.3/4.7	106 Asp βCH
104 Arg NH	2210	3470	5.8	4.4	107 Lys NH
104 Arg δCH_2	480		8.4	7.4	107 Lys δCH_2
104 Arg ϵNH	340	720	8.9	9.3	107 Lys ϵCH_2
105 Asp NH	3120		4.8	3.3	108 Asn NH
105 Asp βCH	4140		nd	4.9	108 Asn βCH
105 Asp βCH′	3200		4.7	5.5	108 Asn βCH′
106 Ala NH	2740	3990	5.2	4.3	109 Ala NH
106 Ala αCH	1740		6.3	5.4	109 Ala αCH
106 Ala βCH_3	600	1810	8.0	7.3	109 Ala βCH_3
107 Asp βCH	3430		4.4	5.2/4.6	110 Asp βCH_2
108 Gly NH	2520	3700	5.5	4.4	111 Gly NH
108 Gly αCH	630		7.9	6.5	111 Gly αCH
108 Gly αCH′	1230		6.9	6.2	111 Gly αCH′
109 Tyr NH	2920	3000	5.1	3.2	112 Phe NH
109 Tyr βCH	2690		5.2	3.8	112 Phe βCH
109 Tyr βCH′	2380		5.6	5.1	112 Phe βCH′
109 Tyr 3,5	1010	2210	7.2	8.2	112 Phe ζC
109 Tyr 2,6	1790	2600	6.2	5.8	112 Phe γC
110 Ile γCH_3	1130		7.0	6.6	113 Ile γCH_3
110 Ile δCH_3	1030		7.2	7.7	113 Ile δCH_3
111 Asp NH	2330	3370	5.7	3.7	114 Asp NH
111 Asp βCH	2710		5.2	6.4/4.7	114 Asp βCH
112 Ala NH	1660		6.3	7.9	115 Ile NH
112 Ala βCH_3	510	2000	8.3	10.2	115 Ile αCH
114 Glu NH	1920		6.1	6.1	117 Glu NH
115 Leu NH	650		7.9	7.2	118 Leu NH
115 Leu δCH_3	370		8.8	10.8	118 Leu δCH_3
115 Leu $\delta CH_3'$	340		8.9	11.2	118 Leu $\delta CH_3'$
115 Leu NH_2	270	710	9.3	9.7	119 Gly NH

and Leu 115 suggest that these protons are protected from solvent and/or are involved in intramolecular hydrogen bond formation.[2] Satyshur et al. (1988) indicate that hydrogen bonds are made to Asp 103, Ala 106, Gly 108, Tyr 109, Ile 110, Asp 111, and Leu 115 (the numbering refers to the peptide sequence), with the strongest hydrogen bond (shortest N···O distance) being made to Gly 108. Thus the correspondence is not perfect, although the smallest value measured for $\Delta\delta/\Delta T$ is also for Gly 108. The temperature coefficient data might also be expected to correlate with the fractional intensities of the amide resonances at higher temperatures (Table II). These reflect the amide proton exchange rate [$f = 1/(1 + k_{ex}T_{1NH})$; O'Neil & Sykes, 1988]: a very slow rate would yield a remaining fractional intensity of 1.0; a very fast rate would result in disappearance of the signal (ratio = 0). Slow amide exchange is often also correlated with lack of solvent exposure and/or hydrogen bonding. However, the correlation between these two sets of measurements is not strong. This certainly indicates that care must be taken in interpreting exchange or temperature coefficient data in terms of a single cause such as hydrogen bonding. In particular, the areas of several resonances seem to decrease rather rapidly between 40° and 50°, which may reflect a change in conformation.

Conclusion

The structure in solution of the metal-bound form of the synthetic calcium-binding loop peptide is very similar to that of the loop in the protein, thereby supporting the use of synthetic peptide analogues to elucidate the basis of calcium affinity and selectivity in calcium-binding proteins.

[2] Intermolecular interactions can be discounted because the chemical shifts of the NH resonances were found to be independent of peptide concentration over the range 3.5–18 mM.

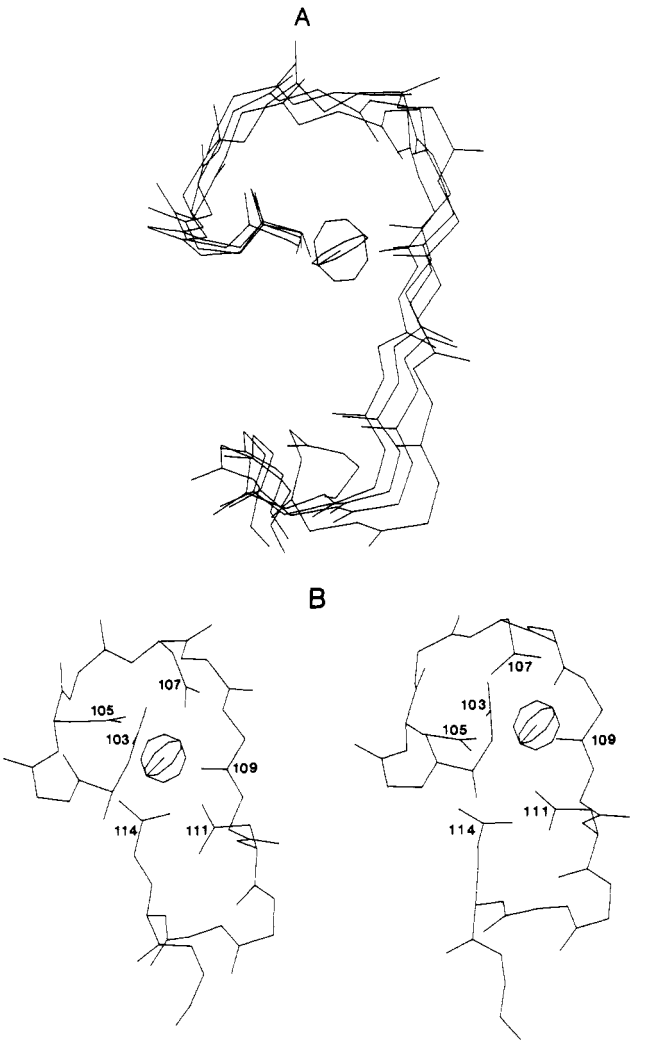

FIGURE 7: (A) Comparison of the conformation of the peptide backbone taken from the X-ray structure and that of three molecular dynamics structures calculated including the NMR distances as pseudo potential energy restraints. The metal ions were superimposed. (B) Comparison of the conformation of the peptide backbone plus liganding residues between the X-ray structure (left) and the energy-minimized average of the three NMR structures (right).

Acknowledgments

We thank R. Lemke for the many hours spent purifying the peptide, M. Nattriss for performing the amino acid analyses of the samples in this study, Dr. W. Paranchych for use of the HPLC equipment, Dr. R. Reid for use of his program MUTATE, N. Strydnaka and Dr. M. N. G. James for helpful discussions and assistance with graphics, Dr. O. Herzberg for helpful discussions and for providing us with the X-ray coordinates of TnC, J. D. Baleja and Dr. J. Moult for help with the energy minimization and molecular graphics calculations, B. Kenney for use of the NMR facilities at Varian Canada, Ottawa, and Dr. H. D. Dettman for help with the NMR software.

References

Barker, W. C., Ketcham, L. K., & Dayhoff, M. O. (1978) in *Atlas of Protein Sequence and Structure* (Dayhoff, M. O., Ed.) Vol. 5, Suppl. 3, The National Biomedical Research Foundation, Silver Spring, MD.

Bax, A., & Drobny, G. (1985) *J. Magn. Reson. 61*, 306–320.

Bloembergen, N. (1957a) *J. Chem. Phys. 27*, 572–573.

Bloembergen, N. (1957b) *J. Chem. Phys. 27*, 595–596.

Borin, G., Pezzoli, A., Marchiori, F., & Peggion, E. (1985) *Int. J. Peptide Protein Res. 26*, 528–538.
Buchta, R., Bondi, E., & Fridkin, M. (1986) *Int. J. Peptide Protein Res. 28*, 289–297.
Bundi, A., & Wüthrich, K. (1979) *Biopolymers 18*, 285–297.
Bystrov, V. F. (1976) *Prog. Nucl. Magn. Reson. Spectrosc. 10*, 41–81.
Cheung, W. Y. (1970) *Biochim. Biophys. Acta 38*, 533–538.
Crippen, G. (1981) in *Chemometrics Research Studies Series* (Bawden, D., Ed.) p 1, Research Studies Press, Wiley, New York.
Derancourt, J., Haiech, J., & Pechère, J.-F. (1978) *Biochim. Biophys. Acta 532*, 373–375.
Deslauriers, R., & Smith, I. C. P. (1980) in *Biological Magnetic Resonance* (Berliner, L., & Reuben, J., Eds.) Vol. 5, pp 243–344, Plenum, New York.
Ebashi, S., Kodama, A., & Ebashi, F. (1968) *J. Biochem. (Tokyo) 64*, 465–477.
Eich, G., Bodenhausen, G., & Ernst, R. R. (1982) *J. Am. Chem. Soc. 104*, 3731–3732.
Gariépy, J., & Hodges, R. S. (1983) *FEBS Lett. 160*, 1–6.
Gariépy, J., Sykes, B. D., Reid, R. E., & Hodges, R. S. (1982) *Biochemistry 21*, 1506–1512.
Gariépy, J., Sykes, B. D., & Hodges, R. S. (1983) *Biochemistry 22*, 1765–1772.
Gariépy, J., Kay, L. E., Kuntz, I. D., Sykes, B. D., & Hodges, R. S. (1985) *Biochemistry 24*, 544–550.
Gariépy, J., Lane, A., Frayman, F., Wilbur, D., Robien, W., Schoolnik, G. K., & Jardetzky, O. (1986) *Biochemistry 25*, 7854–7866.
Havel, T., Kuntz, I. D., & Crippen, G. M. (1983) *Bull. Math. Biol. 45*, 665–720.
Herzberg, O., Moult, J., & James, M. N. G. (1987) *Methods Enzymol. 139*, 610–632.
Kakiuchi, S., & Yamazaki, R. (1970) *Biochim. Biophys. Acta 41*, 1104–1110.
Kanellis, P., Yang, J., Cheung, H. C., & Lenkinski, R. E. (1983) *Arch. Biochem. Biophys. 220*, 530–540.
Kolat, R. S., & Powell, J. E. (1962) *Inorg. Chem. 1*, 293–296.
Kretsinger, R. H. (1980) *CRC Crit Rev. Biochem. 8*, 119–174.
Kretsinger, R. H., & Nockolds, C. E. (1973) *J. Biol. Chem. 248*, 3313–3326.
Lanir, A., & Navon, G. (1972) *Biochemistry 11*, 3536–3544.
Lee, L., & Sykes, B. D. (1980) *Biochemistry 19*, 3208–3214.
Malik, N. A., Anantharamaiah, G. M., Gawish, A., & Cheung, H. C. (1987) *Biochim. Biophys. Acta 911*, 221–230.
Marchiori, F., Borin, G., Chessa, G., Cavaggion, G., Michelin, L., & Peggion, E. (1983) *Hoppe Seyler's Z. Physiol. Chem. 364*, 1019–1028.
Marsden, B. J., Hodges, R. S., & Sykes, B. D. (1987) in *Calcium-Binding Proteins in Health and Disease* (Norman, A. W., Vanaman, T. C., & Means, A. R., Eds.) pp 412–414, Academic Press, San Diego, CA.
Marsden, B. J., Hodges, R. S., & Sykes, B. D. (1988) *Biochemistry 27*, 4198–4206.
Pardi, A., Billter, M., & Wüthrich, K. (1984) *J. Mol. Biol. 180*, 741–781.
Pavone, P. V., Di Nola, A., Andini, S., Ferrara, L., Di Blasio, B., Benedetti, E., & Pucci, P. (1984) *Int. J. Peptide Protein Res. 23*, 454–461.
Piantini, U., Sørensen, O. W., & Ernst, R. R. (1982) *J. Am. Chem. Soc. 104*, 6800–6801.
Rance, M., Sørensen, O. W., Bodenhausen, G., Wagner, G., Ernst, R. R., & Wüthrich, K. (1983) *Biochem. Biophys. Res. Commun. 117*, 479–485.
Reid, R. E., & Hodges, R. S. (1980) *J. Theor. Biol. 84*, 401–444.
Reid, R. E., Clare, D. M., & Hodges, R. S. (1980) *J. Biol. Chem. 255*, 3642–3646.
Reid, R. E., Gariépy, J., Saund, A. K., & Hodges, R. S. (1981) *J. Biol. Chem. 256*, 2742–2751.
Satyshur, K. A., Rao, S. T., Pyzalska, D., Drendel, W., Greaser, M., & Sundaralingam, M. (1988) *J. Biol. Chem. 263*, 1628–1647.
Seamon, K. B., & Kretsinger, R. H. (1983) in *Calcium in Biology* (Spiro T. G., Ed.) p 1, Wiley-Interscience, New York.
Solomon, I. (1955) *Rev. Biol. 99*, 559–565.
Strydnaka, N. C. J., & James, M. N. G. (1989) *Annu. Rev. Biochem. 58*, 951–998.
Sykes, B. D., Hull, W. E., & Snyder, G. H. (1978) *Biophys. J. 21*, 137–146.
Szebenyi, D. M. E., & Moffat, K. (1986) *J. Biol. Chem. 261*, 8761–8777.
Vogt, H.-P., Strassburger, W., Wollmer, A., Fleischhauer, J., Bullard, B., & Mercola, D. (1979) *J. Theor. Biol. 76*, 297–310.
Weber, P. L., Drobny, G., & Reid, B. R. (1985) *Biochemistry 24*, 4549–4552.
Williamson, M. P., & Neuhaus, D. (1987) *J. Magn. Res. 72*, 369–375.
Wüthrich, K. (1986) in *NMR of Proteins and Nucleic Acids*, John Wiley & Sons, New York.